Effects of incomplete mixing on reactive transport in flows through heterogeneous porous media

Elise E. Wright,* David H. Richter, and Diogo Bolster
Department of Civil and Environmental Engineering and Earth Sciences, University of Notre Dame, Notre Dame, Indiana 46556, USA
(Received 10 March 2017; published 8 November 2017)

The phenomenon of incomplete mixing reduces bulk effective reaction rates in reactive transport. Many existing models do not account for these effects, resulting in the overestimation of reaction rates in laboratory and field settings. To date, most studies on incomplete mixing have focused on diffusive systems; here, we extend these to explore the role that flow heterogeneity has on incomplete mixing. To do this, we examine reactive transport using a Lagrangian reactive particle tracking algorithm in two-dimensional idealized heterogeneous porous media. Contingent on the nondimensional Peclet and Damköhler numbers in the system, it was found that near well-mixed behavior could be observed at late times in the heterogeneous flow field simulations. We look at three common flow deformation metrics that describe the enhancement of mixing in the flow due to velocity gradients: the Okubo-Weiss parameter (θ), the largest eigenvalue of the Cauchy-Green strain tensor (λ_C), and the finite-time Lyapunov exponent (Λ). Strong mixing regions in the heterogeneous flow field identified by these metrics were found to correspond to regions with higher numbers of reactions, but the infrequency of these regions compared to the large numbers of reactions occurring elsewhere in the domain imply that these strong mixing regions are insufficient in explaining the observed near well-mixed behavior. Since it was found that reactive transport in these heterogeneous flows could overcome the effects of incomplete mixing, we also search for a closure for the mean concentration. The conservative quantity $\overline{u^2}$, where $u = C_A - C_B$, was found to predict the late time scaling of the mean concentration, i.e., $\overline{C_i} \sim \overline{u^2}$.

DOI: 10.1103/PhysRevFluids.2.114501

I. INTRODUCTION

Chemical reactions are an important factor to consider in many flowing systems [1–5]. A perhaps obvious, but critical feature to recognize in any of these systems is that in order for a reaction to actually occur, the reactants involved in a reaction must first come into contact with each other. Mixing is the process that enables this, and consequently, the mechanism that drives reactions. Given that flows can serve to enhance or attenuate mixing, they can also have a pronounced effect on reactions in a given system.

Incomplete mixing reduces the overall bulk effective reaction rates in fluid systems with mixing-driven chemical reactions. However, the effects of this phenomenon are typically not sufficiently accounted for in existing models, resulting in the overestimation of reaction rates in laboratory experiments and field measurements [6–10]. Incomplete mixing limits the ability of reactants to come into contact, causing slower reaction rates compared to a well-mixed system. A variety of models have been developed and used to address this problem, including probability density function (pdf) closures [11], anomalous transport models [12,13], modified effective kinetics [14], fractional advection-dispersion equations (fADE) [15], moment equations [16], and particle tracking methods [12,13,17,18]. It is important to be able to accurately predict reaction rates, as it can have great consequences in many real world applications, an example being the remediation of contaminants

*ewright4@nd.edu

in groundwater [19–21] and surface flows [1]. Therefore, there is a need to be able to understand and adequately describe these incomplete mixing effects to accurately model reactive transport.

To examine this problem of incomplete mixing, it is common to look at irreversible bimolecular kinetic reactions of the form $A + B \rightarrow P$. This simple bimolecular case has been shown to be the foundation for more complex reactions [22]. Since the focus of this work is on how the solutes A and B mix and react with one another, the product of their reaction will be neglected for simplicity and we have $A + B \rightarrow \emptyset$. In a system where reactions occur with some known rate coefficient k and there are equal initial amounts of A and B distributed uniformly throughout the domain, i.e., $C_A(x,y,t = 0) = C_B(x,y,t = 0) = C_0$, there is a well-known analytical solution for the concentration $C_A(x,y,t) = C_B(x,y,t) = C_0/(1 + kC_0t)$, which scales like t^{-1} at late times [23]. This solution assumes that the system is perfectly well-mixed at all times. In real systems, however, this will generally not be true, particularly in mixing-limited systems where reaction time scales are faster than mixing time scales. This behavior is quantified by a nondimensional Damköhler number (Da), which is defined as the ratio of the diffusion time scale to the reaction time scale [15]. Thus, low Da indicates that mixing (i.e., diffusion) is happening more quickly than reactions and well-mixed behavior is expected. In contrast, high values of Da means that reactions are occurring more quickly than mixing by diffusion and incomplete mixing behaviors can arise. If there is some fluctuation of C_A and C_B about the mean, these fluctuations will become more dominant relative to the mean over time as reactions occur and reduce the mean concentration. These concentration fluctuations will cause reactant solutes to segregate from one another and form patches of only one species, which we refer to as *islands*. Since the reactants must come into contact before a reaction can occur, reactions are limited to the interface between these islands, causing the overall reduction in the amount of reaction that takes place. This is the phenomenon we call incomplete mixing.

This problem has been studied extensively in systems where reactive solutes move purely by diffusion [8,9,16,23–26] and while we are motivated by flows in porous media, this problem has applications as far ranging as physics [26,27], chemistry [28], biology [29], economics [30–32], and social sciences [33]. Under these conditions, the emergence of incomplete mixing leads to a slowdown in reaction and the mean concentration has been shown to scale like $t^{-d/4}$ at late times in these systems, where d is the number of spatial dimensions. This result has been found in theory [24–26], numerical simulations [24–26], and experimental observations [8,9]. The late-time scaling behavior indicates a significant reduction in the overall number of reactions due to the strong effects of incomplete mixing in these systems. Here, mixing occurs by diffusion alone. The natural next step is to examine systems where diffusion driven mixing is modified due to advection in nonuniform flow fields.

The presence of a nonuniform flow field will cause the solutes to mix very differently than they would in a uniform flow field where mixing occurs only by diffusion [34]. This difference is due to the stretching and compression experienced by the fluid as a result of flow heterogeneity [35–37]. Since reactive species need to come into contact for a reaction to actually occur, the different mixing characteristics in these nonuniform fields are also likely to impact reactions. It is expected that mixing will be increased in nonuniform velocity fields, implying that it may also enhance reactions. Many studies have worked to quantify mixing in heterogeneous systems by examining the temporal evolution of global measures of mixing such as the scalar dissipation rate [38–40] and the dilution index [35,38,41]. Metrics such as second centered spatial moments are often used to quantify spreading as well, which when accounted for properly can be tied back to mixing processes [42]. The aforementioned scalar dissipation rate and dilution index are global measures of mixing, but mixing is inherently a local process dictated by local flow features. It is strong local gradients in a velocity field that can cause stretching and compression that in turn influence mixing. To this end, there are also many local flow deformation metrics related to velocity gradients that are used to describe mixing characteristics of the flow field. Previous studies have considered flow deformation metrics such as the Okubo-Weiss parameter [35,43], the largest eigenvalue of the Cauchy-Green strain tensor [43], the finite-size Lyapunov exponent [44], and the finite-time

Lyapunov exponent [43]. These studies tied the flow deformation metrics to mixing and then made potential inferences about reactions, but to date no study explores the link between these velocity gradient metrics and reactive transport. All of these metrics mentioned here that quantify mixing and spreading provide measures that quantify the ability for reactants to collocate. For this reason, it is often argued that they should also serve as strong indicators of the amount of reactions that occur at a given location in a flow; while the arguments seem reasonable, they remain to be tested.

Recently the ideas of incomplete mixing were explored in a simple nonuniform flow, namely linear shear [45]. As in the purely diffusive systems, it was found that incomplete mixing appeared when reactions occurred more quickly than mixing by diffusion and the shear flow [45]. They found, however, a high sensitivity to the additional time scale associated with shear: depending on the strength of the shear, the flow could seemingly overcome the incomplete mixing effects and exhibit the well-mixed scaling behavior at late times [45]. Incomplete mixing was still present in their systems as segregated *islands* of reactants clearly emerged, but the shear fluxes across the island interfaces were sufficiently large that the system would behave as if it were well-mixed, albeit at a slower effective reaction rate. While a lot can be learned from the shear flow case, it is a highly idealized flow and has also been shown to possibly be a limit case as one of the most efficient flows for inducing mixing [38]. The goal of this work is to to take this one step further and apply these concepts to more general nonuniform flows that are more representative of what would be found in real systems. In particular we will focus on flows through two-dimensional idealized heterogeneous porous media.

While the focus of this work is on incomplete mixing in flows through idealized heterogeneous porous media in two dimensions, in principle the ideas presented here should be applicable to any incompressible and steady nonuniform flow. Will these heterogeneous flows attenuate the effects of incomplete mixing? How will the results compare to existing studies on purely diffusive systems and pure shear flow? Where are reactions most likely to happen? We address these questions using a Lagrangian-based reactive transport model, and thus extend recent work that has been performed in more idealized settings.

II. NUMERICAL MODEL

The governing equation for transport in our system is the advection-dispersion-reaction equation (ADRE). For our two reactive species, A and B, the ADRE is

$$\frac{\partial C_i}{\partial t} = D\nabla^2 C_i - \mathbf{v}\cdot\nabla C_i - kC_A C_B, \quad i = A, B, \tag{1}$$

where C_i is the concentration [mol L^{-2}], D is the local dispersion coefficent [L^2T^{-1}], which is assumed to be constant, $\mathbf{v}(\mathbf{x})$ is the incompressible velocity [LT^{-1}], and k is the reaction rate constant [L^2 mol$^{-1}T^{-1}$]. It is well-known that random walks can be used to numerically simulate the advection-dispersion equation (ADE), and these ideas have been extended to include reactions [46]. This particular Lagrangian particle tracking algorithm has been used to study reactive transport in homogeneous [23,47] and heterogeneous advection fields [45,48]. Solving the ADRE with this Lagrangian method requires that the solutes A and B are divided into particles that each represent some finite mass, m_p. Time is discretized into time steps of size Δt, and at each time step the amount of reaction that takes place is determined and the nonreacted particles continue to move by random walk. Full details of this method and generalizations, including rigorous demonstrations that they converge and represent Eq. (1), are available from multiple sources, including Refs. [23,46–50], and so we only provide a brief description here.

A. Particle tracking algorithm in a single time step

The algorithm involves marching the system through time via discrete time steps. Here we illustrate briefly the procedure for one time step from t_1 to t_2, where $t_2 = t_1 + \Delta t$. It is a two-step process analogous to operator splitting.

1. Step 1—Reaction

First, it is determined whether or not each particle will react in the given timestep based on their probability of reaction. The probability of reaction is dependent on both the probability that particles will come into contact, $P_{\text{collocation}}$, and the kinetics of the reaction once two particles have collocated, $P_{\text{react|coll}}$. It is defined as

$$P_{\text{reaction}} = P_{\text{collocation}} P_{\text{react|coll}}. \tag{2}$$

The probability of collocation, $P_{\text{collocation}}$, is the probability that a particle pair separated by a distance s will collocate over time step Δt. $P_{\text{react|coll}}$ is the probability that two particles will react with one another given that they have come into contact [23,46]. The probability of reaction is defined as

$$P_{\text{reaction}} = \frac{k m_p}{8\pi D} \exp\left(-\frac{s^2}{8D\Delta t}\right), \tag{3}$$

where m_p is the particle mass [mol]. For a specific A particle, the probability of reaction is calculated between that particle and all B particles within a particular radius of its location at t_1. This radius is chosen such that the probability of reaction for that A particle with any B particle outside this radius is less than 10^{-6}, which has been shown to provide acceptable results [47], i.e.,

$$r = \sqrt{-8D\Delta t \log\left(\frac{8\pi D\Delta t P_{\text{reaction}}}{P_{\text{react|coll}}}\right)}, \tag{4}$$

with $P_{\text{reaction}} = 10^{-6}$. A random number ξ_i is generated from $U(0,1)$ for each AB particle pair. If for any AB pair $P_{\text{reaction},i} > \xi_i$, then the A and B particles react and are removed from the system according to the reaction $A + B \rightarrow \emptyset$. If multiple B particles meet the requirements for reaction with a single A particle, then the AB pair with the highest value of $R = P_{\text{reaction},i} - \xi_i$ is chosen for reaction. If none of the AB pairs meet the requirement for reaction, then the particular A particle does not react and we move on to the next A particle. This process is repeated until the reaction algorithm has cycled through all of the A particles and determined which ones, if any, will react. The particle searching process in this step of the algorithm was made more computationally efficient through the implementation of a k-dimensional tree. This reduces the complexity from an $O(N^2)$ process to $O(N \log N)$. Once the reaction step is completed, we then move on to the random walk component of the algorithm.

2. Random walk

After the first substep is complete, particles move by random walk in both $\mathbf{x}(x,y)$ directions according to Langevin equation,

$$\mathbf{x}(t_2) = \mathbf{x}(t_1) + \mathbf{v}(t_1)\Delta t + \sqrt{2D\Delta t}\,\boldsymbol{\xi}, \tag{5}$$

where $\boldsymbol{\xi} \sim N(0,1)$. Thus, the particle locations are updated by both advection and a diffusive step. In the advective step, $\mathbf{v}$ indicates the velocity of the particle, obtained from the prescribed flow fields, described in the following. The last term reflects a random jump experienced by the particle due to diffusion with zero mean and a variance of $2D\Delta t$.

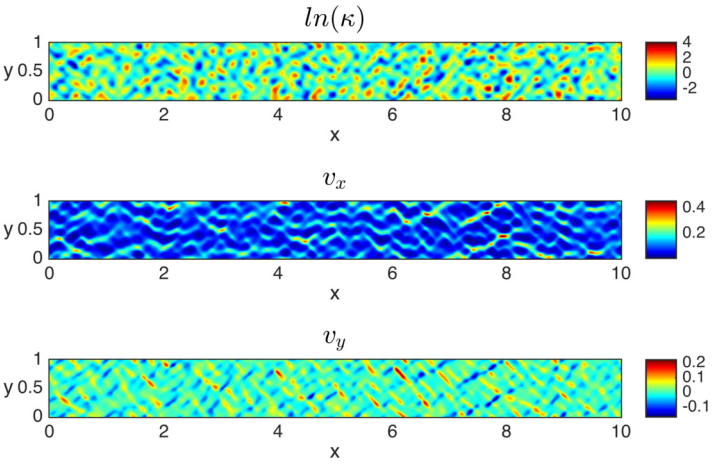

FIG. 1. (Top) The natural logarithm of the permeability field, $\ln(\kappa)$. (Middle) Horizontal velocity v_x and (Bottom) vertical velocity v_y. Lengths have been normalized to the domain extent in the y direction.

B. Flow fields

The flow fields studied in this work are idealized two-dimensional heterogeneous porous media. The permeability fields are generated from the superposition of randomly shifted periodic waves with integer numbers of wavelengths that fit within the defined domain and are scaled to a specified variance. The permeability fields are periodic on all sides and characterized by a correlation length $l_{\ln\kappa}$ and variance $\sigma^2_{\ln\kappa}$. These lognormal random Gaussian-correlated fields are the standard model used to describe heterogeneous porous media [51,52]. Darcy's law, $\mathbf{v}(x,y) = \frac{\kappa}{\mu}\nabla p$, coupled with incompressibility $\nabla \cdot \mathbf{v} = 0$, subject to a uniform pressure drop in the horizontal direction of flow, is then solved using finite differences to obtain the flow field. A sample permeability field and the corresponding flow field is shown in Fig. 1. Due to the nature of Darcy's law, we can rescale the flow velocity values to any desired mean velocity.

III. MEAN CONCENTRATION

We initially have equal amounts of solutes A and B in our system, i.e.,

$$\overline{C}_A(x,y,t=0) = \overline{C}_B(x,y,t=0) = C_0, \tag{6}$$

where the overbars denote volume averages over the spatial domain. Since A and B react in a 1:1 reaction, this means that $\overline{C}_A(t)=\overline{C}_B(t)$ at all times. To generate as close to uniform an initial condition in concentration, the particles representing solutes A and B are initially distributed randomly with uniform probability across the entire domain. For our setup, we initially have $N = 500\,000$ particles of each species with $2N$ total particles in the system. Note that this will in fact not result in a perfectly uniform concentration field due to small subscale fluctuations. It is precisely these small-scale fluctuations that amplify, resulting in incomplete mixing effects. If these fluctuations were not present the system would likely remain perfectly well mixed, but we argue that perfect mixing is untenable in real systems. We examine the behavior of the mean concentration in time as it is a measure of the amount of reaction that has taken place in our system. As discussed in the introduction, it is known that if the system is well mixed, the mean concentration will evolve as

$$C_{i,\mathrm{wm}}(x,y,t) = \overline{C}_{i,\mathrm{wm}}(t) = \frac{C_0}{(1+kC_0t)} \sim t^{-1} \quad \text{(at late times)}, \tag{7}$$

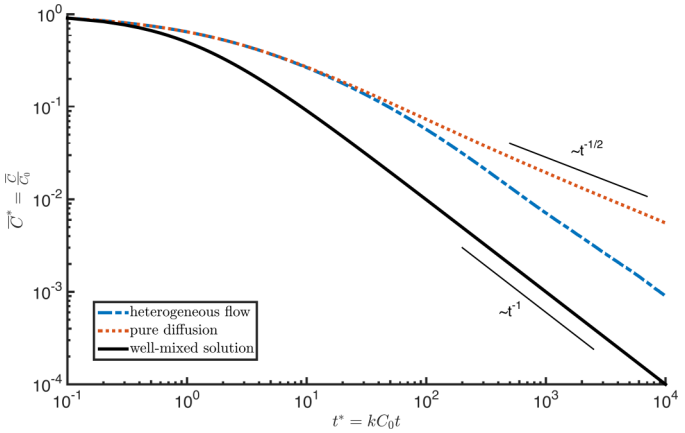

FIG. 2. The black line corresponds to the well-mixed solution for the mean concentration and scales like t^{-1} at late times. The red line is the result for the mean concentration in a purely diffusive system and scales as $t^{-1/2}$ at late times. The blue line corresponds to the mean concentration from our simulation in an idealized heterogeneous porous medium with Pe = 1200 and Da = 14 400. At late times, our model results for this particular heterogeneous field scales as if it were almost well-mixed.

and that a purely diffusive system will scale as $t^{-d/4}$ at late times when incomplete mixing arises. Since we are considering a two-dimensional $d = 2$ system, a late time scaling of $t^{-1/2}$ is expected. For illustrative purposes, Fig. 2 shows results for a representative system that we consider. On it are shown the analytical solution Eq. (7) of the mean concentration under perfect mixing and the simulation results for both the mean concentration in a purely diffusive system and a system with the heterogeneous flow field shown in Fig. 1. A constant local dispersion coefficient of $D = 10^{-5}$ and a reaction rate of $k = 10$ were used for both simulations. The flow field in Fig. 1 has $l_{\ln\kappa} = 0.12$, $\sigma^2_{\ln\kappa} = 1$, and $\overline{v}_x = 0.1$, where $\overline{v}_x$ is the mean velocity in the x direction. Figure 3 shows the particle locations at four points in time throughout the heterogeneous flow field simulation and demonstrates how the *islands* grow over time. It was found that at early times the mean concentration for the heterogeneous system is in agreement with the purely diffusive case. Then at some point in time, the system accelerates relative to the diffusive case and in terms of scaling with time it begins to behave as if it were nearly well-mixed, i.e., $\sim t^{-1}$, but with a lower effective reaction rate due to the continued presence of incomplete mixing. This transition from purely diffusive behavior to a nearly well-mixed scaling occurs when $t \approx l_{\ln\kappa}/\overline{v}_x$. This corresponds to the characteristic time when particles have had the opportunity to move through regions of different permeabilities (i.e., traverse a correlation length with the mean velocity), which explains why this is the time when the effects of the nonuniform flow begin to impact the results for the mean concentration (see Fig. 3).

Several cases were studied looking at a variety of heterogeneous flow fields, Damköhler (Da) numbers, and Peclet (Pe) numbers. Figure 4 shows the mean concentration versus time for the cases with varying Peclet and Damköhler numbers that were examined in this study. The diffusive Damköhler number is defined here as $\mathrm{Da} = \frac{kC_0 l^2_{\ln\kappa}}{D}$. As mentioned in the Introduction, the Damköhler number is a ratio of a transport time scale (in this case diffusion) to the reaction time scale. The Peclet number is defined as $\mathrm{Pe} = \frac{\overline{v}_x l_{\ln\kappa}}{D}$ and describes the ratio of advective transport to diffusive transport. As shown in Fig. 4, if Da is held the same, the simulation results will display more well-mixed behavior with increasing Pe. This is because advection dominates with high Pe and the enhanced mixing due to the nonuniformity of the flow field will dampen the incomplete mixing effects. In contrast, holding Pe the same and increasing Da will lead to a stronger emergence of incomplete mixing behavior. This is because large Da indicates that reactions are happening faster than mixing can bring reactants together. The representative case shown in Figs. 2 and 3 is a system with Pe = 1200 and Da = 14 400. We will return to this representative case later in our discussion.

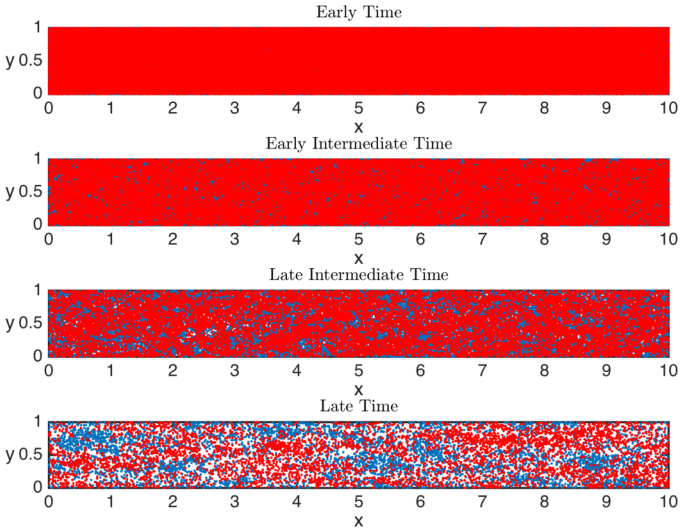

FIG. 3. The A and B particle locations for a system with Pe = 1200 and Da = 14 400 are shown at an early time ($t^* = 12$), early intermediate time ($t^* = 54.1$), late intermediate time ($t^* = 155.4$), and late time ($t^* = 630.6$). It is observed that the islands grow in size over time, demonstrating the presence of incomplete mixing in the system.

In this work we will address two main questions regarding the behavior of the mean reactant concentration. First, can we explain the nearly well-mixed scaling that was observed at late times in Fig. 2? Specifically can we attribute this to regions of strong mixing as characterized by velocity gradient based flow deformation metrics? Then we ask: Given a flow field, can we predict the late-time behavior of the mean concentration without having to solve a full reactive transport problem?

IV. CONNECTING FLOW DEFORMATION METRICS AND REACTIONS

A. Where do reactions occur?

As discussed in the previous section, the results of our reactive transport simulations through heterogeneous flows showed that these systems could, depending on their Peclet and Damköhler numbers, behave as if they were nearly well mixed at late times, but with a reduced overall reaction rate due to incomplete mixing. Metrics based on flow deformation provide information about the enhancement of mixing due to the flow field. Since mixing drives chemical reactions in these systems, we explore three different flow deformation metrics and determine whether there is any connection between them and reactions. The goal here is to see if high mixing regions as indicated by these flow deformation metrics can help explain the nearly well-mixed behavior that was observed in our simulations at late times.

The flow deformation metrics we consider are all based on the velocity gradient tensor $\mathbf{E} = \nabla \mathbf{v}$, where the diagonal terms describe stretching and compressing effects from the flow field and the off-diagonal terms represent shear and rotation. The Okubo-Weiss parameter illustrates the balance between these diagonal and off-diagonal terms and is defined as

$$\theta(\mathbf{x}) = -4 \det(\mathbf{E}), \tag{8}$$

as discussed in Refs. [35,43]. It was found that there is a direct correlation between the evolution of mixing from a point source, as quantified by the entropy based dilution index, and the Okubo-Weiss parameter [35], suggesting that this metric could be important when studying mixing and reactions. The Lagrangian deformation gradient tensor, $\mathbf{F}$, represents the deformation experienced by a fluid

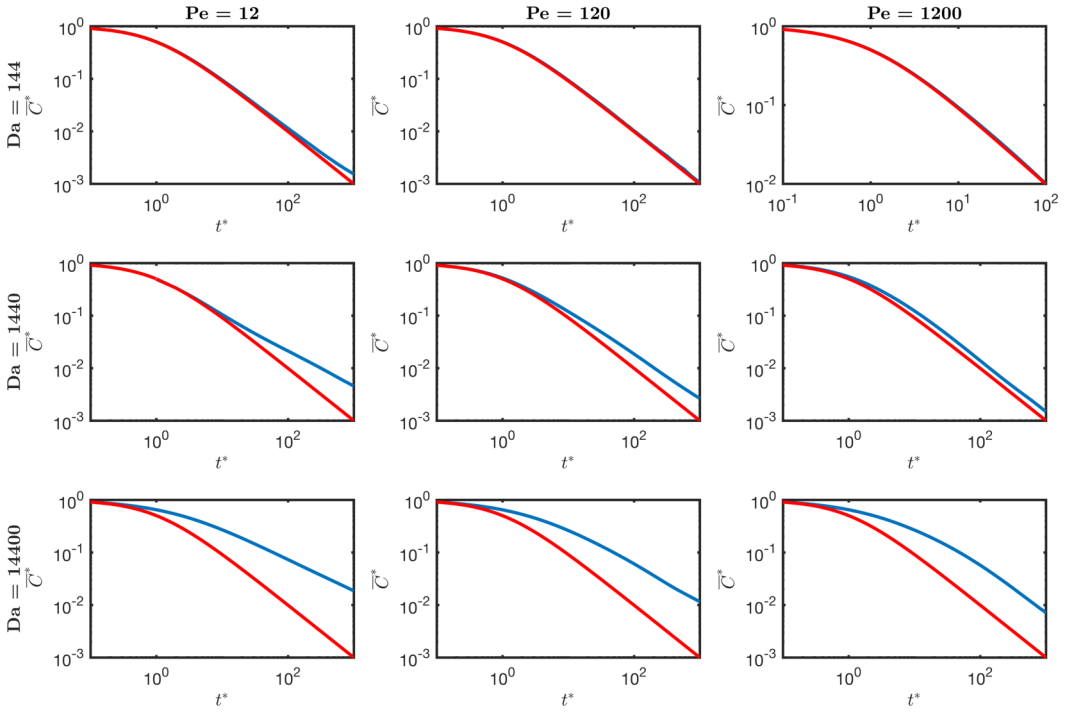

FIG. 4. The mean concentration vs. time is shown for the simulation results of nine cases with different Peclet and Damköhler numbers. The red lines are the well-mixed solution defined in Eq. (7) and the blue lines are the simulation results for heterogeneous flow field cases at the specified Peclet and Damköhler numbers.

parcel at a specific point over a given amount of time. Since rotation does not contribute to mixing, the right Cauchy-Green strain tensor removes its contribution and is given by

$$\mathbf{C}(\mathbf{x}) = \mathbf{F}^T\mathbf{F}. \tag{9}$$

The largest eigenvalue of the Cauchy-Green strain tensor, λ_C, quantifies the strength of the deformation [43]. The final metric based on flow topology that we look at is the finite-time Lyapunov exponent (Λ), defined as

$$\Lambda(\mathbf{x}) = \frac{\ln\left[\lambda_C(\mathbf{x})\right]}{2\Delta t}. \tag{10}$$

Here we examine the impact of the Okubo-Weiss parameter (θ), the largest eigenvalue of the Cauchy-Green strain tensor (λ_C), and the finite-time Lyapunov exponent (Λ) on reactive transport. We are motivated by the fact that in a heterogeneous flow there is a demonstrable connection between the collocation density, which drives reactions, and θ, λ_C, and Λ [43]. Here we will directly compare these flow deformation metrics to reactions and see if they correlate to the regions where reactions are most likely to occur in our system.

B. Simulation results

Ten realizations of our reactive transport simulation were performed for the same flow field for each case of varying Peclet and Damköhler numbers considered in this study and the location of every reaction that took place in each simulation was recorded. Our goal here is to determine if there is a connection between regions of high mixing potential, as quantified by the flow deformation metrics, and the number of reactions that actually occurs at any given location. Based on previous

TABLE I. Correlation coefficients between reaction numbers and flow deformation metrics for each of the nine cases with different Peclet and Damköhler numbers. N_r is the number of reactions obtained from a two-dimensional histogram of reaction locations for ten realizations.

	Pe = 12	Pe = 120	Pe = 1200
	$\rho_{X,Y}$	$\rho_{X,Y}$	$\rho_{X,Y}$
Da = 144	$\rho_{N_r,\theta} = -0.0020$	$\rho_{N_r,\theta} = 0.0380$	$\rho_{N_r,\theta} = 0.0365$
	$\rho_{N_r,\lambda_C} = 0.0208$	$\rho_{N_r,\lambda_C} = 0.0740$	$\rho_{N_r,\lambda_C} = 0.0596$
	$\rho_{N_r,\Lambda} = 0.0384$	$\rho_{N_r,\Lambda} = 0.0972$	$\rho_{N_r,\Lambda} = 0.0639$
	$\rho_{X,Y}$	$\rho_{X,Y}$	$\rho_{X,Y}$
Da = 1440	$\rho_{N_r,\theta} = 0.0147$	$\rho_{N_r,\theta} = 0.0167$	$\rho_{N_r,\theta} = 0.0725$
	$\rho_{N_r,\lambda_C} = 0.0324$	$\rho_{N_r,\lambda_C} = 0.0511$	$\rho_{N_r,\lambda_C} = 0.1085$
	$\rho_{N_r,\Lambda} = 0.0373$	$\rho_{N_r,\Lambda} = 0.0672$	$\rho_{N_r,\Lambda} = 0.1281$
	$\rho_{X,Y}$	$\rho_{X,Y}$	$\rho_{X,Y}$
Da = 14 400	$\rho_{N_r,\theta} = 0.0006$	$\rho_{N_r,\theta} = 0.0429$	$\rho_{N_r,\theta} = 0.0342$
	$\rho_{N_r,\lambda_C} = 0.0123$	$\rho_{N_r,\lambda_C} = 0.0631$	$\rho_{N_r,\lambda_C} = 0.0508$
	$\rho_{N_r,\Lambda} = 0.0127$	$\rho_{N_r,\Lambda} = 0.0521$	$\rho_{N_r,\Lambda} = 0.0557$

arguments [43], it might be expected that regions with strong mixing potential will bring the reactants together more efficiently. Thus, if the high mixing regions increase the likelihood of reactants to collocate, it is expected that higher amounts of reactions will take place there.

Our initial check to see if there was any relationship between reaction locations and the flow deformation metrics was to calculate the correlation coefficient, which for generic variables X and Y is defined as

$$\rho_{X,Y} = \frac{K_{X,Y}}{\sigma_X \sigma_Y}, \tag{11}$$

where $K_{X,Y}$ is the covariance of X and Y, and σ_X and σ_Y are the standard deviations of X and Y, respectively. The three flow deformation metrics θ, λ_C, and Λ were calculated on a grid defined over the entire domain of the system. The location of every reaction that occurred throughout each simulation was stored on the same grid. The correlation coefficient was calculated by directly comparing the numbers of reactions that occurred in a given location for all times to the flow deformation metrics at the same location as defined by the grid. The results of this for all cases are shown on Table I. The correlation coefficients between the number of reactions and each of the flow deformation metrics were found to have low values for all cases, implying that there is no significant correlation between them. At first sight this suggests that the arguments of increased likelihood of reaction presented in Ref. [43] are wrong, but a closer inspection is warranted before making such a conclusion. To this end, we must consider some conditional statistics.

Since low correlation coefficients were found for all cases shown in Table I, we now shift our focus back to our representative case with Pe = 1200 and Da = 14 400 and increase the number of realizations to 100 for a more in-depth analysis. The two-dimensional histogram of reaction locations over 100 realizations and the flow deformation metrics calculated for this system are shown in Fig. 5. Figure 6 shows scatterplots of each of the deformation metrics and the corresponding number of reactions for every location on the defined grid, displaying the low correlation coefficients found in Table I. Although the correlation coefficient indicates that there is no significant correlation between the amount of reaction and the flow deformation metrics, we found that the highest mixing regions specified by these metrics did correspond to regions that had a large number of reactions. To explore this further, we define a threshold number of reactions, τ, and look at the flow deformation metrics in regions where the number of reactions that took place is at or above this threshold. The mean value of a specific flow deformation metric β (where $\beta = \theta$, λ_C, or Λ) at locations with numbers of

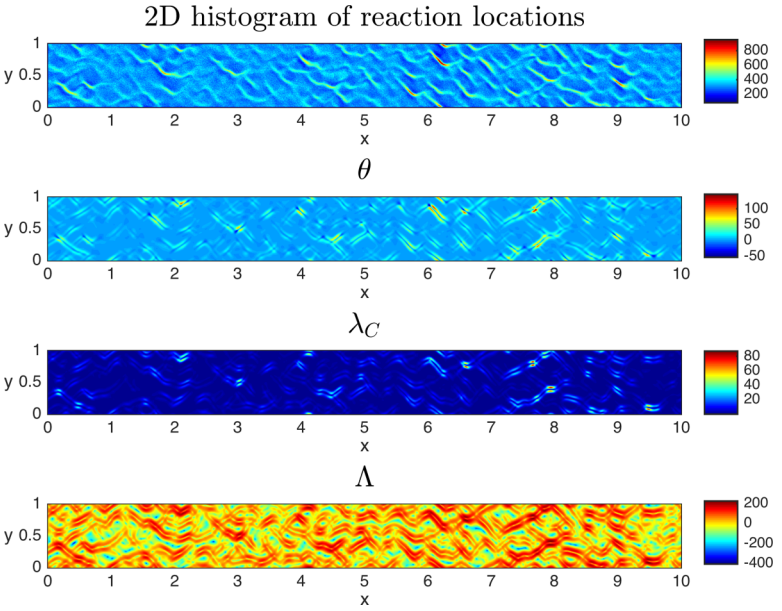

FIG. 5. (a) The two-dimensional histogram of reaction locations for 100 realizations of the Pe = 1200 and Da = 14 400 case. Every time a reaction occurs, the location of the reaction is recorded. (b) The corresponding fields of the Okubo-Weiss parameter (θ), (c) λ_C, and (d) the finite-time Lyapunov exponent (Λ) are shown.

reactions above the threshold τ is defined by

$$\overline{\beta}_{\geqslant\tau}(\tau) = \frac{\sum_{i=1}^{N_{\mathrm{gp}}} \beta_i H[N_{r_i} - \tau]}{\sum_{i=1}^{N_{\mathrm{gp}}} H[N_{r_i} - \tau]}, \tag{12}$$

where N_{gp} is the number of grid points, β_i is the value of the flow deformation metric at the ith grid point, N_{r_i} is the number of reactions that took place at the ith grid point, and $H[N_{r_i} - \tau]$ is the Heaviside step function. Plots of $\overline{\beta}_{\geqslant\tau}$ versus τ for each of the flow deformation metrics are shown in Fig. 7. These figures demonstrate that by filtering locations in the domain based on whether or not the number of reactions that occurred there is above a specified threshold, the strongest mixing regions as indicated by the flow deformation metrics did indeed have more reactions. That is, to observe the behaviors anticipated by Ref. [43] statistics must be looked at from a conditional perspective. The reason that the correlation coefficients indicated a weak correlation between the

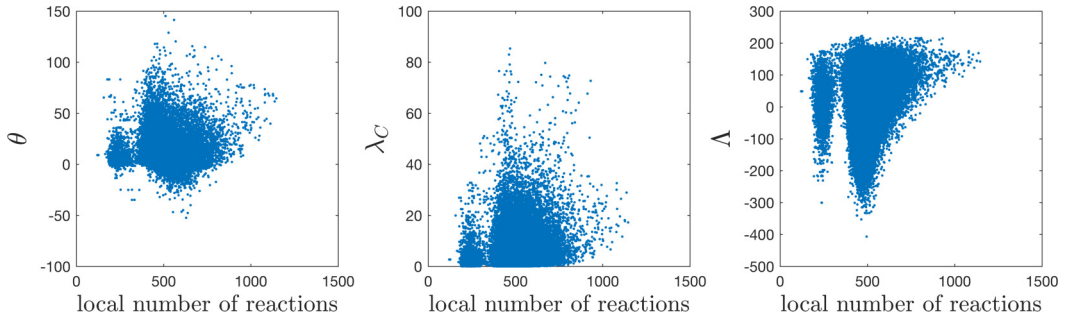

FIG. 6. A scatterplot of the local values of θ, λ_C, and Λ and the number of reactions at the same locations for the Pe = 1200 and Da = 14 400 case.

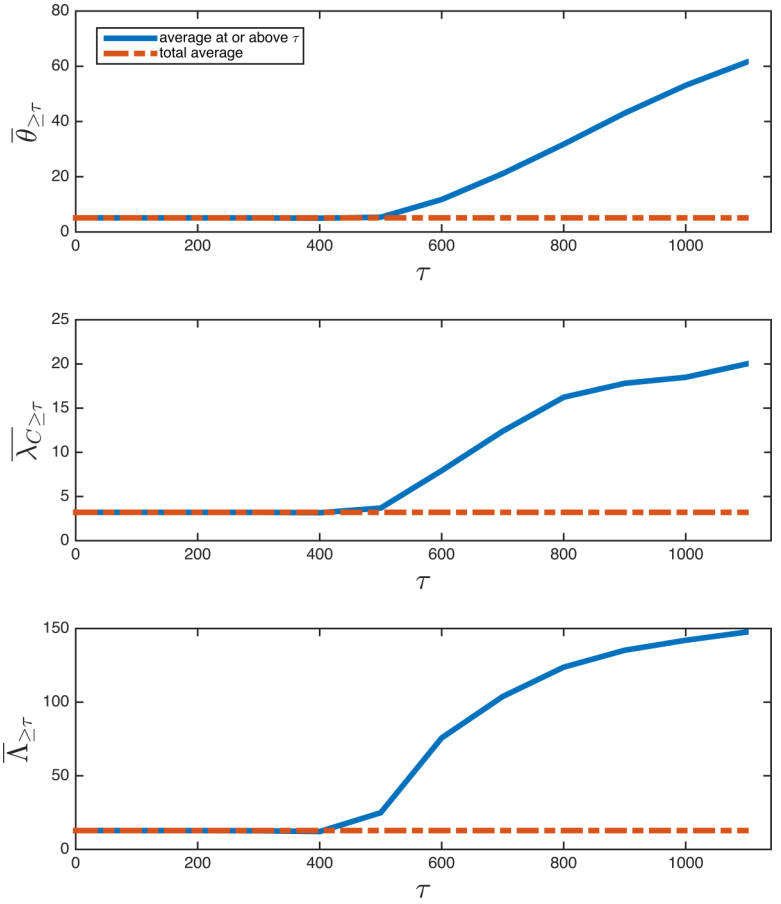

FIG. 7. The average θ, λ_C, and Λ values at locations where the amount of reactions that have occurred is above the threshold τ indicated on the x-axis for the Pe $= 1200$ and Da $= 14\,400$ case.

flow deformation metrics and reaction numbers is that these high mixing regions make up a very small portion of the domain and only a small fraction of the total amount of reactions took place in these regions. This means that there is a relationship between flow topology and reactions, but there are so many reactions happening everywhere else in the domain that the impact of these high mixing regions on reactions as a whole is negligible in a global sense. For this reason, the regions with strong mixing defined by flow deformation metrics cannot sufficiently explain the well-mixed behavior observed at late times in our simulation. It should be noted that these results are for reactive transport in two-dimensional heterogeneous porous media and may not be universally true for real three-dimensional systems. As was found for the two-dimensional case, we expect that there will be no significant correlation between flow topology metrics and reactions in three-dimensions. Further work would need to be done to verify this and other metrics of flow topology may need to be considered in the three-dimensional case.

V. CLOSURE FOR THE LATE-TIME BEHAVIOR OF THE MEAN CONCENTRATION

The initial condition for our transport simulations is to have equal amounts of A and B distributed randomly and uniformly throughout the domain. Due to the stochastic nature of this initial condition,

we separate the concentration into its mean and fluctuation,

$$C_i(\mathbf{x},t) = \overline{C_i}(t) + C_i'(\mathbf{x},t), \tag{13}$$

where $\overline{C_i}$ is the volume average over the domain and C_i' is the fluctuation from that mean. By substituting Eq. (13) into Eq. (1) and averaging, an equation for the rate of change of the mean concentration in time is found to be

$$\frac{\partial \overline{C_i}}{\partial t} = -k\overline{C_i}^2 - k\overline{C_A' C_B'}. \tag{14}$$

The expected behavior of the mean concentration over time can be explained using a dominant balance argument. At early times, the concentration fluctuations will be small compared to the mean, so the second-order fluctuation term, $\overline{C_A' C_B'}$, can be neglected. This leads to the well-mixed solution and indicates that at early times our simulation results should behave as if they were well-mixed. This is indeed true as seen in Fig. 2, where the simulation results for both a purely diffusive system and a system with a heterogeneous flow field agree with the well-mixed solution at very early times. At late times when reactions have removed most of the A and B particles from the domain, the mean concentration changes more slowly in time so the $\frac{\partial \overline{C_i}}{\partial t}$ term can be neglected and a dominant balance between the other two terms in Eq. (14) emerges. Thus, the mean concentration is expected to scale as

$$\overline{C_i} \sim \sqrt{-\overline{C_A' C_B'}} \tag{15}$$

at late times. If it is known how $\overline{C_A' C_B'}$ scales at late times, then the late time behavior of the mean concentration will be known as well. Our goal is to be able to predict the scaling of the mean concentration given any flow field without needing to perform a reactive transport simulation and measure it. To do this, we need a closure for $\overline{C_A' C_B'}$.

A. Closure Approach 1—Peak of the Green's function

Previous studies, based on the method of moments, have suggested that a closure for $\overline{C_A' C_B'}$ can be found by calculating the peak of the Green's function [15,16,45,53]. These studies showed that

$$\overline{C_A' C_B'} \sim -G(\mathbf{x} = \mathbf{x_{peak}}, t). \tag{16}$$

While this result is theoretical, it is built using many assumptions which may be dubious for a system with nonuniform advection (e.g., statistical stationarity and the initial anticorrelation of second order moments). Nonetheless, given the great success of these methods across so many examples we test it here. To measure $G(\mathbf{x} = \mathbf{x_{peak}}, t)$, we simulated the evolution of a pulse of conservative particles in our heterogeneous flow field shown in Fig. 1 and measured the peak. Due to the nonstationary nature of the domain, multiple starting locations were considered. In all cases, while at early times differences were observed, it was found that at late times $\mathrm{G}(\mathbf{x} = \mathbf{x_{peak}}, \mathrm{t}) \sim t^{-1.2}$, which suggests that we should expect the mean concentration to scale as $\sim t^{-0.6}$. This indicates that the late time behavior of the mean concentration in our heterogeneous fields should be closer to the purely diffusive scaling than it is to the well-mixed scaling. By examining the results in Fig. 2, however, this is clearly not true. This can likely be attributed to the fact that the peak of the Green's function is dependent on the initial condition since our system is not homogeneous. Therefore, the peak of the Green's function closure may not be general and cannot be used as a closure for this system.

B. Closure Approach 2—Conservative component $\overline{u^2}$

To find a closure for $\overline{C_A' C_B'}$, we define a conservative component

$$u = C_A - C_B. \tag{17}$$

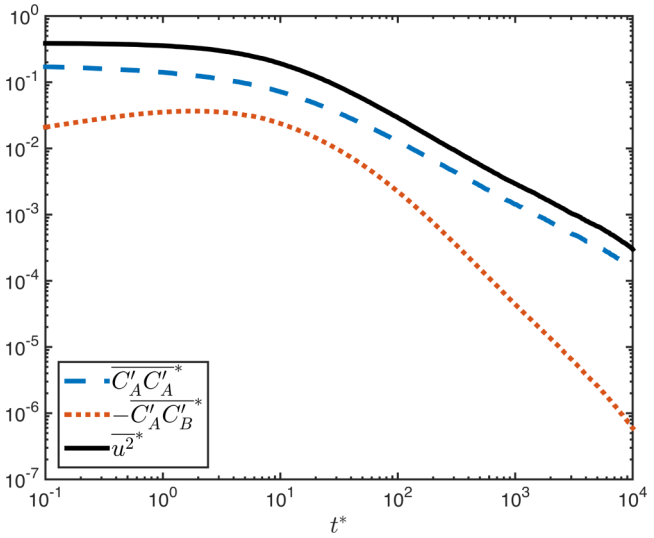

FIG. 8. The evolution of $\overline{C'_A C'_A}$, $\overline{C'_A C'_B}$, and $\overline{u^2}$ in time for a system with Pe = 1200 and Da = 14 400. At late times, $\overline{u^2}$ scales like $\overline{C'_A C'_A}$. The quantities $\overline{C'_A C'_A}$, $\overline{C'_A C'_B}$, and $\overline{u^2}$ have been nondimensionalized by C_0^2.

This conservative quantity has been widely used in studies of reactive transport systems [24,26,54,55]. It is called the conservative component, because Eq. (1) can be written for $i = \mathrm{A}$ and $i = \mathrm{B}$ and the ADRE for $i = \mathrm{B}$ can be subtracted from the ADRE for $i = \mathrm{A}$ to obtain the following conservative equation for u:

$$\frac{\partial u}{\partial t} = D\nabla^2 u - \mathbf{v} \cdot \boldsymbol{\nabla} u. \tag{18}$$

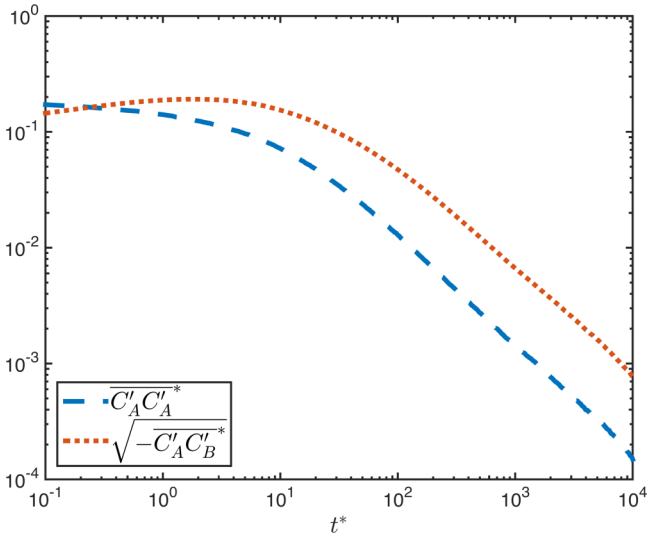

FIG. 9. The evolution of $\sqrt{-\overline{C'_A C'_B}}$, and $\overline{C'_A C'_A}$ in time for a system with Pe = 1200 and Da = 14 400. At late times, $\overline{C'_A C'_A}$ scales like $\sqrt{-\overline{C'_A C'_B}}$.

From Eqs. (13) and (17), we can show

$$\overline{u^2} = 2\overline{C'_A C'_A} - 2\overline{C'_A C'_B}. \tag{19}$$

This means that the conservative quantity $\overline{u^2}$ is related to the reactive quantities $\overline{C'_A C'_A}$ and $\overline{C'_A C'_B}$. We examine the behavior of $\overline{u^2}$ in time, with the goal of learning about the late time scaling of $\overline{C'_A C'_B}$ and, ultimately, via Eq. (15) the mean concentration.

1. Simulation results

Using the same particle tracking algorithm described previously we can calculate u and thus $\overline{u^2}$. All three terms in Eq. (19) are plotted as a function of time in Fig. 8. It is clear from Fig. 8 that at late times,

$$\overline{u^2} \sim \overline{C'_A C'_A}. \tag{20}$$

This means that if the conservative quantity $\overline{u^2}$ is measured, then the late time behavior of the reactive quantity $\overline{C'_A C'_A}$ is known.

Recall that the term whose behavior we are interested in is $\overline{C'_A C'_B}$, because it will give us the late time behavior of the mean concentration. We find that at late times that the relationship between the behavior of $\overline{C'_A C'_A}$ and $\overline{C'_A C'_B}$ is given by

$$\overline{C'_A C'_A} \sim \sqrt{-\overline{C'_A C'_B}}. \tag{21}$$

This is shown in Fig. 9. Equation (21) contradicts assumptions made in the moment argument of Ref. [16], which led to the Green's function closure, possibly explaining why it failed here.

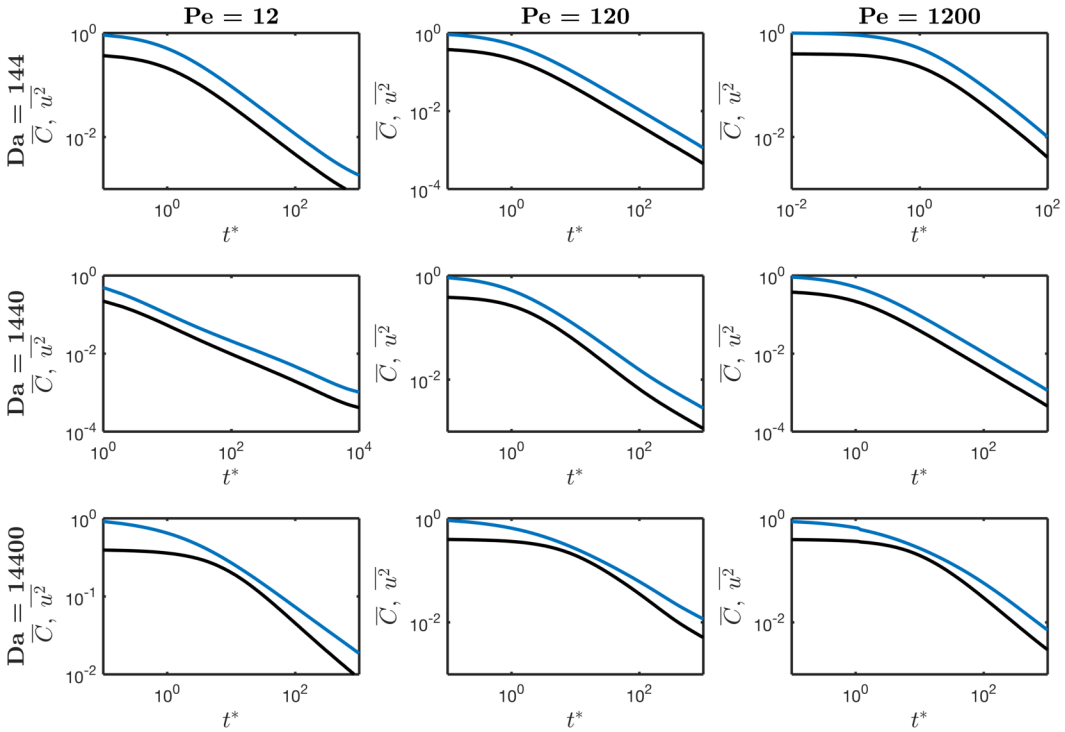

FIG. 10. The evolution of $\overline{C_i}$ and $\overline{u^2}$ in time. $\overline{C_i}$ is given by the blue line and the black line is $\overline{u^2}$. At late times, $\overline{C_i} \sim \overline{u^2}$.

Interestingly, the same behavior is observed in purely diffusive systems and this exact scaling can be clearly seen in the figures of Ref. [23] but went unnoticed in that work. This result has been found consistently in our simulation results for reactive transport across a broad range of parameter space in both our heterogeneous flow fields and purely diffusive systems. Finally, by combining Eqs. (21), (20), and (15), we find that at late times we expect

$$\overline{C_i} \sim \overline{u^2}. \tag{22}$$

Thus, if we know the late time behavior of $\overline{u^2}$ we also know the behavior of the mean concentration. This late time scaling behavior was found to be consistent for the variety of Peclet and Damköhler numbers examined in this study. The evolution of the mean concentration $\overline{C_i}$ and $\overline{u^2}$ in time for these cases is shown in Fig. 10. This suggests that we can solve a reactive transport problem by understanding the conservative one.

VI. CONCLUSION

We have studied reactive transport in heterogeneous flows with the goal of understanding how the nonuniformity of the flow field impacts mixing and reactions. Specifically, we were interested in observing the effects of the heterogeneous velocity field on incomplete mixing and determining where in the flow reactions are most likely to take place.

To study this problem, we examined bimolecular reactions of the form $A + B \rightarrow \emptyset$ using a Lagrangian reactive particle tracking method. This numerical model was used to investigate systems over a range of Peclet and Damköhler numbers. In systems with low Da, diffusion leads to mixing at faster rates than reactions occur and so behaviors close to well-mixed are observed. Additionally, with high Pe the enhanced mixing that arises due to the stretching and deformation associated with the nonuniform velocity field causes the system to behave more well mixed. For these high Pe cases, the mean concentration always returns to a near well-mixed scaling at late times even with the presence of incomplete mixing. In the regime of low Pe and high Da, strong incomplete mixing behavior is present since reactions occur faster than mixing can bring reactants together. Specific focus is placed on the case of $\mathrm{Pe} = 1200$ and $\mathrm{Da} = 14\,400$, since it is representative of incomplete mixing behavior in these inhomogeneous settings. At early times for this setup a deviation from the well-mixed solution is observed due to the emergence of incomplete mixing. At some later point in time, when the particles have had a chance to travel through regions of varying permeability, the system returns to a near well-mixed scaling due to the enhanced mixing by the nonuniform flow field.

To identify where reactions are most likely to occur, we looked at three flow deformation metrics that describe the enhancement of mixing due to velocity gradients in the flow: the Okubo-Weiss parameter (θ), the largest eigenvalue of the Cauchy-Green strain tensor (λ_C), and the finite-time Lyapunov exponent (Λ). Our goal was to determine whether or not these metrics could explain the near-well mixed behavior that was observed at late times for the $\mathrm{Pe} = 1200$ and $\mathrm{Da} = 14\,400$ case. High mixing regions defined by these flow deformation metrics were found to have much higher numbers of reactions than other locations in the system. However, these strong mixing regions make up a relatively small portion of our domain and the vast majority of the total number of reactions occurred elsewhere. This tells us that while the regions of high mixing potential quantified by these flow deformation metrics do indicate locations where larger numbers of reactions are expected to occur, they are insufficient in explaining the near well-mixed behavior that was observed at late times in these heterogeneous flow fields.

After understanding that the inhomogeneous flow fields can overcome incomplete mixing effects, a closure for the mean concentration equation was sought so that late time behavior could be predicted based entirely on conservative transport. It was found that the late-time scaling behavior of the mean concentration of a reactive transport simulation can be predicted from the conservative quantity $\overline{u^2}$, where $u = C_A - C_B$. Specifically, based on a combination of dominant balance arguments and an

empirical relationship seen throughout all of the simulations performed in this study, we find that $\overline{C_i} \sim \overline{u^2}$. While we have been able to show this empirically across a broad and relevant range of parameter space, further work needs to be done to explain this behavior in a rigorous and theoretical manner as it suggests that previous closure arguments may make invalid assumptions.

This study examined reactive transport in a two-dimensional idealized system; however, real systems are, of course, three-dimensional. While valuable information can be learned from the two-dimensional case and a large number of studies on mixing and reactions in porous media focus on two-dimensional flows [e.g., 35,36,38,40,42,43,45,52], additional concerns will arise regarding dilution, mixing, and reactions when these ideas are extended to three dimensions. Dilution will be increased due to the added spatial dimension [41] and mixing will change due to the possibility of twisting streamlines [56–58]. These differences in dilution and mixing will have an impact on reactions. Since there was no significant correlation between flow topology metrics and reactions in two dimensions, we expect that the same will be true for the three-dimensional case as well although continued work would be required to verify this.

In summary, it was found that the nonuniformity of the flow in our idealized two-dimensional heterogeneous porous media could, depending on the nondimensional Peclet and Damköhler numbers, enhance mixing enough to overcome the effects of incomplete mixing in our systems. Flow deformation metrics based on velocity gradients did indicate where high numbers of reactions could be expected, but the impact of this is insignificant for our system as there are many more reactions happening elsewhere in the domain. Finally, it was found that the scaling of the mean concentration at late times can be predicted from the conservative quantity $\overline{u^2}$.

ACKNOWLEDGMENTS

We acknowledge funding from the National Science Foundation Grants No. EAR-1351625, No. EAR-1417264, and No. EAR-1446236.

[1] P. Guerra, C. Gonzalez, C. Escauriaza, G. Pizarro, and P. Pasten, Incomplete mixing in the fate and transport of arsenic at a river affected by acid drainage, Water Air Soil Pollut. **227**, 73 (2016).

[2] S. A. Levin and L. A. Segel, Hypothesis for origin of planktonic patchiness, Nature **259**, 659 (1976).

[3] F. J. Molz and M. A. Widdowson, Internal inconsistencies in dispersion-dominated models that incorporate chemical and microbial kinetics, Water Resour. Res. **24**, 615 (1988).

[4] M. Taillefert and J.-F. Gaillard, Reactive transport modeling of trace elements in the water column of a stratified lake: Iron cycling and metal scavenging, J. Hydrol. **256**, 16 (2002).

[5] T. Tel, A. de Moura, C. Grebogi, and G. Karolyi, Chemical and biological activity in open flows: A dynamical system approach, Phys. Rep. **413**, 91 (2005).

[6] C. M. Gramling, C. F. Harvey, and L. C. Meigs, Reactive transport in porous media: A comparison of model prediction with laboratory visualization, Environ. Sci. Technol. **36**, 2508 (2002).

[7] V. Kapoor, C. T. Jafvert, and D. A. Lyn, Experimental study of a bimolecular reaction in Poiseuille flow, Water Resour. Res. **34**, 1997 (1998).

[8] E. Monson and R. Kopelman, Observation of Laser Speckle Effects and Nonclassical Kinetics in an Elementary Chemical Reaction, Phys. Rev. Lett. **85**, 666 (2000).

[9] E. Monson and R. Kopelman, Nonclassical kinetics of an elementary $A + B \rightarrow C$ reaction-diffusion system showing effects of a speckled initial reactant distribution and eventual self-segregation: Experiments, Phys. Rev. E **69**, 021103 (2004).

[10] D. S. Raje and V. Kapoor, Experimental study of bimolecular reaction kinetics in porous media, Environ. Sci. Technol. **34**, 1234 (2000).

[11] G. Chiogna and A. Bellin, Analytical solution for reactive solute transport considering incomplete mixing within a reference elementary volume, Water Resour. Res. **49**, 2589 (2013).

[12] Y. Edery, H. Scher, and B. Berkowitz, Particle tracking model of bimolecular reactive transport in porous media, Water Resour. Res. **46**, W07524 (2010).
[13] Y. Edery, A. Guadagnini, H. Scher, and B. Berkowitz, Reactive transport in disordered media: Role of fluctuations in interpretation of laboratory experiments, Adv. Water Resour. **51**, 86 (2013).
[14] X. Sanchez-Vila, D. Fernàndez-Garcia, and A. Guadagnini, Interpretation of column experiments of transport of solutes undergoing an irreversible bimolecular reaction using a continuum approximation, Water Resour. Res. **46**, W12510 (2010).
[15] D. Bolster, P. de Anna, D. A. Benson, and A. M. Tartakovsky, Incomplete mixing and reactions with fractional dispersion, Adv. Water Resour. **37**, 86 (2012).
[16] A. M. Tartakovsky, P. de Anna, T. Le Borgne, A. Balter, and D. Bolster, Effect of spatial concentration fluctuations on effective kinetics in diffusion-reaction systems, Water Resour. Res. **48**, W02526 (2012).
[17] Z. Alhashmi, M. J. Blunt, and B. Bijeljic, Predictions of dynamic changes in reaction rates as a consequence of incomplete mixing using pore scale reactive transport modeling on images of porous media, J. Contam. Hydrol. **179**, 171 (2015).
[18] D. Ding, D. A. Benson, A. Paster, and D. Bolster, Modeling bimolecular reactions and transport in porous media via particle tracking, Adv. Water Resour. **53**, 56 (2013).
[19] C. Knutson, A. Valocchi, and C. Werth, Comparison of continuum and pore-scale models of nutrient biodegradation under transverse mixing conditions, Adv. Water Resour. **30**, 1421 (2007).
[20] K. U. Mayer, S. G. Benner, and D. W. Blowes, Process-based reactive transport modeling of a permeable reactive barrier for the treatment of mine drainage, J. Contam. Hydrol. **85**, 195 (2006).
[21] C. I. Steefel, D. J. DePaulo, and P. C. Lichtner, Reactive transport modeling: An essential tool and a new research approach for the Earth sciences, Earth Planet. Sci. Lett. **240**, 539 (2005).
[22] D. T. Gillespie, Stochastic simulation of chemical kinetics, Annu. Rev. Phys. Chem. **58**, 35 (2007).
[23] A. Paster, D. Bolster, and D. A. Benson, Connecting the dots: Semi-analytical and random walk numerical solutions of the diffusion-reaction equation with stochastic initial conditions, J. Comput. Phys. **263**, 91 (2014).
[24] K. Kang and S. Redner, Scaling Approach for the Kinetics of Recombination Processes, Phys. Rev. Lett. **52**, 955 (1984).
[25] A. A. Ovchinnikov and Ya. B. Zeldovich, Role of density fluctuations in bimolecular reaction kinetics, Chem. Phys. **28**, 215 (1978).
[26] D. Toussaint and F. Wilczek, Particle—Antiparticle annihilation in diffusive motion, J. Chem. Phys. **78**, 2642 (1983).
[27] S. A. Rice, *Diffusion-Limited Reactions*, Comprehensive Chemical Kinetics Vol. 25 (Elsevier, Amsterdam, 1985).
[28] E. Kotomin and V. Kuzovkov, *Modern Aspects of Diffusion-Controlled Reactions: Cooperative Phenomena in Bimolecular Processes*, Comprehensive Chemical Kinetics Vol. 34 (Elsevier, Amsterdam, 1996).
[29] J. D. Murray, *Mathematical Biology: I. An Introduction* (Springer, New York, 2002).
[30] D. Becherer and M. Schweizer, Classical solutions to reaction-diffusion systems for hedging problems with interacting Itô and point processes, Ann. Appl. Probab. **15**, 1111 (2005).
[31] J. Fort and V. Mendéz, Reaction-diffusion waves of advance in the transition to agricultural economics, Phys. Rev. E **60**, 5894 (1999).
[32] C.-Z. Li and K.-G. Löfgren, Renewable resources and economic sustainability: A dynamic analysis with heterogeneous time preferences, J. Environ. Econ. Manag. **40**, 236 (2000).
[33] F. Schweitzer, *Brownian Agents and Active Particles: Collective Dynamics in the Natural and Social Sciences* (Springer, Berlin/Heidelberg, 2007).
[34] M. Dentz, T. Le Borgne, A. Englert, and B. Bijeljic, Mixing, spreading and reaction in heterogeneous media: A brief review, J. Contam. Hydrol. **120-121**, 1 (2011).
[35] F. P. J. de Barros, M. Dentz, J. Koch, and W. Nowak, Flow topology and scalar mixing in spatially heterogeneous flow fields, Geophys. Res. Lett. **39**, L08404 (2012).
[36] T. Le Borgne, M. Dentz, and E. Villermaux, Stretching, Coalescence, and Mixing in Porous Media, Phys. Rev. Lett. **110**, 204501 (2013).

[37] S. W. Weeks and G. Sposito, Mixing and stretching efficiency in steady and unsteady groundwater flows, Water Resour. Res. **34**, 3315 (1998).
[38] D. Bolster, M. Dentz, and T. Le Borgne, Hypermixing in linear shear flow, Water Resour. Res. **47**, W09602 (2011).
[39] N. B. Engdahl, T. R. Ginn, and G. E. Fogg, Scalar dissipation rates in nonconservative transport systems, J. Contam. Hydrol. **149**, 46 (2013).
[40] T. Le Borgne, M. Dentz, D. Bolster, J. Carrera, J.-R. de Dreuzy, and P. Davy, Non-Fickian mixing: Temporal evolution of the scalar dissipation rate in heterogeneous porous media, Adv. Water Resour. **33**, 1468 (2010).
[41] P. K. Kitanidis, The concept of the dilution index, Water Resour. Res. **30**, 2011 (1994).
[42] P. de Anna, J. Jimenez-Martinez, H. Tabuteau, R. Turuban, T. Le Borgne, M. Derrien, and Y. Méheust, Mixing and reaction kinetics in porous media: An experimental pore scale quantification, Environ. Sci. Technol. **48**, 508 (2014).
[43] N. B. Engdahl, D. A. Benson, and D. Bolster, Predicting the enhancement of mixing-driven reactions in nonuniform flows using measures of flow topology, Phys. Rev. E **90**, 051001 (2014).
[44] N. Kleinfelter, M. Moroni, and J. H. Cushman, Application of the finite-size Lyapunov exponent to particle tracking velocimetry in fluid mechanics experiments, Phys. Rev. E **72**, 056306 (2005).
[45] A. Paster, T. Aquino, and D. Bolster, Incomplete mixing and reactions in laminar shear flow, Phys. Rev. E **92**, 012922 (2015).
[46] D. A. Benson and M. M. Meerschaert, Simulation of chemical reaction via particle tracking: Diffusion-limited versus thermodynamic rate-limited regimes, Water Resour. Res. **44**, W12201 (2008).
[47] A. Paster, D. Bolster, and D. A. Benson, Particle tracking and the diffusion-reaction equation, Water Resour. Res. **49**, 1 (2013).
[48] D. A. Benson, T. Aquino, D. Bolster, N. Engdahl, C. V. Henri, and D. Fernàndez-Garcia, A comparison of Eulerian and Lagrangian transport and nonlinear reaction algorithms, Adv. Water Resour. **99**, 15 (2017).
[49] D. A. Benson and D. Bolster, Arbitrarily complex chemical reactions on particles, Water Resour. Res. **52**, 1 (2016).
[50] D. Bolster, A. Paster, and D. Benson, A particle number conserving Lagrangian method for mixing-driven reactive transport, Water Resour. Res. **52**, 1 (2016).
[51] R. Ababou and L. W. Gelhar, in *Dynamics of Fluids in Hierarchical Porous Media*, edited by J. H. Cushman (Academic Press, San Diego, CA, 1990), Chap. 14.
[52] B. Zinn and C. F. Harvey, When good statistical models of aquifer heterogeneity go bad: A comparison of flow, dispersion, and mass transfer in connected and multivariate Gaussian hydraulic conductivity fields, Water Resour. Res. **39**, 1051 (2003).
[53] A. Paster and D. Bolster, The effect of initial spatial correlations on late time kinetics of bimolecular irreversible reactions, Physica A **391**, 4654 (2012).
[54] M. De Simoni, J. Carrera, X. Sánchez-Vila, and A. Guadagnini, A procedure for the solution of multicomponent reactive transport problems, Water Resour. Res. **41**, W11410 (2005).
[55] G. Zumofen, J. Klafter, and M. F. Shlesinger, Breakdown of Ovchinnikov-Zeldovich Segregation in the $A + B \rightarrow 0$ Reaction under Levy Mixing, Phys. Rev. Lett. **77**, 2830 (1996).
[56] G. Chiogna, M. Rolle, A. Bellin, and O. A. Cirpka, Helicity and flow topology in three-dimensional anisotropic porous media, Adv. Water Resour. **73**, 134 (2014).
[57] G. Chiogna, O. A. Cirpka, M. Rolle, and A. Bellin, Helical flow in three-dimensional nonstationary anisotropic heterogeneous porous media, Water Resour. Res. **51**, 261 (2015).
[58] O. A. Cirpka, G. Chiogna, M. Rolle, and A. Bellin, Transverse mixing in three-dimensional nonstationary anisotropic heterogeneous porous media, Water Resour. Res. **51**, 241 (2015).